- **Published on: Catalysis Today 195 (2012) 44-53.**
  http://dx.doi.org/10.1016/j.cattod.2012.04.025

Zr-SBA-15 Acid Catalyst: Optimization of the Synthesis and Reaction Conditions for Biodiesel Production from Low-grade Oils and Fats

J.A. Melero[1]*, L.F. Bautista[1], J. Iglesias[2], G. Morales[1], R. Sánchez-Vázquez[1]

[1]Department of Chemical and Environmental Technology, ESCET
Universidad Rey Juan Carlos, Móstoles, 28933, Spain

[2]Department of Chemical and Energy Technology, ESCET
Universidad Rey Juan Carlos, Móstoles, 28933, Spain

*to whom correspondence should be addressed

Tel: +34 91 488 73 99

Fax: +34 91 488 70 68

e-mail: juan.melero@urjc.es

Abstract

The production of biodiesel by methanolysis of highly acidic crude palm oil has been optimized for the Zr-SBA-15 heterogeneous acid catalyst. A dual optimization procedure has been carried out using surface response methodology and selecting the yield towards fatty acid methyl esters (FAMEs) as main response factor. Selected target variables for the optimization were: acidity of the synthesis media, zirconium loading, ageing temperature (all three for the synthesis of the catalyst); and temperature, methanol to oil molar ratio, catalyst loading (for the reaction tests). Quadratic equations were obtained for both models and their statistical analysis led to the optimal conditions for Zr-SBA-15 synthesis (0.67 N HCl media concentration, 130ºC ageing temperature, 10 Si/Zr molar ratio), and for the transesterification reaction conditions (209ºC, 12.45 wt% catalyst loading, 45.8 methanol to oil molar ratio). Under these optimized conditions FAME yield reached 92 mol% after 6 h. Additionally, reusability tests revealed that the optimized Zr-SBA-15 catalyst displays an excellent reaction stability, being fully regenerated after calcination at 450ºC. Moreover, the high catalytic activity and stability achieved with crude palm oil is retained when using waste cooking oil (WCO) or low-grade fats such as category-1 fat, waste lard and mixed fats, leading to FAME yields over 90% after 6 hours, for each raw material, and with acidities in the final product lower than 2.5 mg KOH per gram.

Keywords: FAME, biodiesel, Zr-SBA-15, transesterification, surface response analysis, low-grade oils and fats.

1. Introduction

The production of biodiesel through triglycerides transesterification with methanol is usually carried out in the presence of homogeneous alkalis (NaOH, KOH) as catalysts because of their low price, high availability and excellent catalytic performance. There are, however, important drawbacks associated to their use with high free fatty acids (FFAs)-containing oil sources, such as the formation of soaps which complicate the separation of final products [1]. This trouble is even worse when certain amount of water is present, since the hydrolysis of formed fatty acid methyl esters (FAMEs) yields new FFAs back-feeding the above side reaction. The presence of FFAs additionally leads to some alkaline catalyst consumption, which needs to be compensated by the addition of higher amounts of catalyst [2]. Therefore, FFA content in feedstock for industrial biodiesel production is a critical parameter that is usually limited below 2 wt% [3]. This fact obliges to the use of expensive high-grade oils and fats, such as refined vegetable oils. As alternative, acid catalysts, though less active than base catalyst in this reaction, allow treating high-FFA raw materials because of their ability to catalyze both esterification and transesterification reactions avoiding soap formation [4]. If a heterogeneous acid catalyst is used, further advantages can be found such as catalyst easy recovery and reusability. This is an important benefit which considered together with the lower price of the low-grade FFA-containing feedstock has the potential to improve the overall profitability of biodiesel production process [5]. Reported heterogeneous acid catalysts for biodiesel production comprise a large variety of active phases such as sulfated [6] and mixed metal oxides [7] (mainly zirconia), supported polyanions [8], sulfonic acid-based organic resins and mesostructured materials [9], etc. Several advantages and disadvantages can be

described for each, and apparently none of them displays the combination of high catalytic activity and reutilization properties demanded by such transesterification reaction. Superacid solids like sulfated metal oxides display rather high catalytic activity [6], though quite low stability since sulfate ions (the acid promoter) easily leach from the surface of the catalyst under reaction conditions [10]. In contrast, sulfonic acid-functionalized materials, either resins or mesostructured silica based-solids, evidence strong stability of the catalytic sites. They, however, undergo deactivation phenomena either by the entanglement of the large alkyl chains of fatty acids within the polymeric matrix or by non-reversible strong adsorption of organic molecules over the sulfonic acid sites [11]. In the latter case, the use of calcination as regenerating treatment is not an option because of the organic nature of the catalytic site.

Zirconium-containing mesostructured SBA-15 silica (Zr-SBA-15) has been reported to display an excellent catalytic activity in acid-driven reactions [12], good stability and easy regeneration through calcination. All these properties, together with the open pore structure characteristic of SBA-15 materials, which reduces mass transfer limitations [13], seem to match the requirements for a solid acid catalyst to be used in biodiesel production [5]. Several authors have reported the synthesis of Zr-SBA-15 materials through different synthesis pathways, such as microwave heating [14] or synthesis media pH adjusting methods [15], and starting from different zirconium precursors [16]. In this sense, we have recently reported an alternative synthesis method for the preparation of Zr-SBA-15 materials based on a direct synthesis procedure using zirconocene dichloride as precursor [17]. This methodology, previously described for Ti-SBA-15 materials [18], allows exerting a direct influence on the control of the accessibility of the final supported metal species, enhancing the

catalytic activity thereof [19]. We have also shown that Zr-SBA-15 materials prepared through such a procedure display good catalytic activity in FAME production by methanolysis of highly acidic crude palm oil, accompanied by high stability and reusability after calcination [17]. These results have prompted us to continue this research line through the optimization of both the catalyst synthesis variables and the reaction conditions. Both optimizations have been aimed to maximize the catalytic activity using the yield to fatty acid methyl esters (FAMEs) as response factor, and were carried out by means of surface response methodology [20]. In this way, once the optimal synthesis procedure was achieved we proceeded to optimize the reaction conditions. Finally, the optimized Zr-SBA-15 catalyst has been tested in the processing of different low-quality oleaginous feedstocks under the best reaction conditions.

2. Materials and Methods

2.1. Materials

Zr-SBA-15 mesostructured materials were prepared from tetraethylorthosilicate (TEOS, Aldrich) and zirconocene dichloride (Cp_2ZrCl_2, ABCR) as silicon and zirconium precursors, respectively. The structure-directing agent was the block copolymer Pluronic P-123 (PEO_{20}-PPO_{70}-PEO_{20}, Aldrich). For the dual optimization, crude palm oil (Gran Velada, Zaragoza, Spain) and methanol (Scharlab, Spain) were used as substrates, without previous purification. Animal fats used as comparative low-grade biodiesel feedstocks in the present work were obtained as follows: category-1 fat; lard and mixed fat –consisting of a mixture of low-grade chicken, pig and beef fats sold for the preparation of animal feeds– were acquired from Ibergrasa S.A (Madrid, Spain); and waste cooking oil (WCO) was obtained from

the waste-management facility of Biogras S.L. (Madrid, Spain), treated by a simple filtration procedure to remove suspended solids. The most relevant properties of each feedstock are listed in Table 1.

2.2. Synthesis of Zr-SBA-15 materials

Zirconocene dichloride was used as metal precursor in the synthesis of Zr-SBA-15 materials, following a similar procedure to that previously reported for Ti-SBA-15 [18]. In a typical synthesis, Pluronic 123 (4 g) was dissolved in an aqueous solution of HCl (125 mL at the specified HCl concentration) at room temperature. Upon complete dissolution, zirconocene dichloride was added at the desired silicon to zirconium molar ratio. The resultant suspension was stirred for 3 h and then heated to 40ºC. TEOS (8.63 g) was added to the synthesis media under vigorous stirring, which continued for 20h at 40ºC. The resultant suspension was hydrothermally aged at the desired temperature under static conditions for 24 h. The materials were finally recovered by filtration and air-dried overnight. Surfactant was removed by calcination at 450ºC (5 h in air).

2.3. Characterization techniques

The textural properties of the catalysts were evaluated through N_2 adsorption-desorption isotherms recorded at 77 K in a Micromeritics Tristar 3000 unit. Surface area values were calculated from isotherm data using the B.E.T. method and pore size distributions were obtained through the B.J.H. method using a Harkins-Jura type equation specifically fitted for SBA-15 materials [22]. Total pore volume was assumed to be that recorded at p/p_0 = 0.985. Structural ordering was evaluated by means of low-angle X-ray powder diffraction (XRD) on a Philips X´Pert diffractometer using the Cu Kα line in the 2θ angle range from 0.6º to 5.0º with a step size of 0.02º. The presence of crystalline domains of Zr and/or Si species was determined by high-angle

XRD analysis, in the 2θ angle range from 5.0º to 50.0º (step size of 0.04º). Bulk zirconium contents were determined by Inductively Coupled Plasma-Optical Emission Spectroscopy (ICP-OES). Acidity of the solid samples was determined by ammonia temperature programmed desorption in a Micromeritics 2910 (TPD/TPR) equipment fitted with a TCD detector. Calcined samples were outgassed prior to their analysis under a helium flow (50 NmL·min−1) using a heating rate of 15ºC·min^{-1} up to 560ºC and kept at this temperature for 30 min. After cooling down to 60ºC, an ammonia flow of 35 NmL·min^{-1} was passed through the sample for 30 min. The physically-adsorbed ammonia was removed by flowing helium at 60ºC for 90 min. The chemically-adsorbed ammonia was determined by increasing the temperature up to 550ºC with a heating rate of 15ºC·min^{-1}, maintaining this temperature for 30 min.

2.4. Catalytic tests

The transesterification of crude palm oil with methanol and Zr-SBA-15 materials as a catalyst, was carried out in a 25 mL stainless-steel autoclave (Autoclave Engineers) fitted with a temperature controller, mechanical stirrer and a pressure gauge to monitor the reaction conditions. For every assay, crude palm oil, methanol and catalyst were positioned together inside the reactor vessel before setting up the temperature and stirring conditions (2000 rpm). For the optimization of the synthesis variables of Zr-SBA-15 materials, the reaction conditions were fixed as follows: 200ºC reaction temperature, 10 wt% catalyst loading, and 30:1 methanol to oil molar ratio. On the other hand, for the optimization of the reaction conditions the temperature, catalyst loading and methanol to oil molar ratio were varied as indicated in the discussion. For all the optimization catalytic experiments, the system was allowed to react for 3 hours and afterwards the reactor was cooled down in an ice-water bath. Reaction media was

filtered to recover the catalysts and the remaining methanol was removed in a rotary evaporator under vacuum to obtain the so-called FAME phase (including the produced FAMEs as well as remaining glycerides, FFAs and other non-reacted oily molecules). Analysis of this phase was carried out by means of ^{1}H NMR to evaluate the FAME yield on a molar basis according to the method described by Gelbard [23] using a Varian Mercury Plus 400 unit. For the experiments with different raw materials (low-grade fats and oils), the optimized Zr-SBA-15 catalyst and reaction conditions were used.

2.5. Experimental design and optimization

Response surface methodology was used to optimise the yield of FAME from crude palm oil using Zr-SBA-15 catalysts though both the optimization of the synthesis of the catalyst and the reaction conditions. For the optimization of the synthesis conditions three independent synthesis variables (factors) were selected: the silicon to zirconium molar ratio of the starting synthesis gel (X_1), the hydrochloric acid concentration of the synthesis medium (X_2), and the temperature of the hydrothermal ageing step (X_3). Table 2 lists the range of the values for the selected synthesis parameters and the corresponding levels of the factors. The selected ranges and levels are based on preliminary experimental results [17]. A face-centred central composite design consisting of 18 experiments was performed. The full design comprised 8 (2^3) factorials points (vertexes), 6 star points (face centers) and 4 central point replicas.

On the other hand, for the optimization of the reaction conditions temperature (X_4), catalyst loading (X_5) and methanol to oil molar ratio (X_6) were selected as experimental factors. The range and levels of each factor, both in coded and real units, are given in Table 3. Catalyst loading values are presented as wt% based on the initial

amount of palm oil. Again, the levels of the studied reaction conditions are based on preliminary experimental results [17], and a full factorial central composite design with three-factors was used to set up the experimental design. The complete design consisted of 18 experiments containing 8 factorial points (2^3), 6 star points (star distance, $\alpha = \pm 1.68$) and 4 central point replicates.

All experiments were carried out in a randomized order to minimize the effect of unexplained variability in the observed response. Experimental data were analyzed by response surface methodology using a second-order polynomial equation:

(eq. 1),

where Y is the response (yield to FAME, mol%) and β_0, β_i, β_{ii} and β_{ij} are the regression coefficients of intercept, linear, quadratic and binary interactions, respectively. X_i and X_j are the independent factors. To confirm the parameter estimation and for the sake of the model fitting, an analysis of variance (ANOVA) was performed. The analysis of statistical significance was based on the total error criteria with a confidence level of 95.0%.

3. Results and Discussion

3.1. Optimization of Zr-SBA-15 synthesis conditions

Enhancing the catalytic properties of Zr-SBA-15 materials involves the modification of key synthesis parameters affecting the final properties of the catalytic solid. Since the presence of metal species is the responsible for the catalytic activity of Zr-SBA-15 materials, the final zirconium loading was selected as variable for study. In addition, owing to its effect not only on the incorporation but also on the speciation of

the Zr catalytic sites, the acidity of the synthesis media was also considered as a factor for the optimization study [24]. Finally, and bearing in mind its effect both on the zirconium incorporation and the textural properties, the ageing temperature was considered as the third factor to be evaluated [25]. Therefore, these three synthesis variables were varied according to a factorial design of experiments in order to build a predictive mathematical model using the yield to FAME as optimizing response. Table 4 shows the experimental face-centred cube design including the catalytic results as well as the most relevant physicochemical properties of each synthesised material.

The experimental catalytic results were used to fit a quadratic model whose mathematical expression including the regression coefficients corresponding to significant factors and interactions (at 95% confidence level) is as follows:

$$Y = 61.37 - 2.61 \cdot X_1 - 1.36 \cdot X_2 + 6.08 \cdot X_3 + 1.38 \cdot X_1 \cdot X_2 - 1.50 \cdot X_2 \cdot X_3 - 2.85 \cdot X_2^2 - 2.15 \cdot X_3^2 \quad \text{(eq. 2)},$$

where Y is the response and represents the Yield to FAME expressed as mol%. The coded independent factors (X_i) adopt values between -1 and +1 corresponding to the analyzed ranges. The mathematical model shown in eq. 2 is only valid within the experimental region explored and cannot be used to extrapolate results out of it. The response was simultaneously optimized with respect to all three factors. ANOVA of the quadratic regression model demonstrated that it is significant at a confidence level <95%. The value of the regression coefficient, $r^2 = 0.9447$, indicated a high degree of correlation between the experimentally-observed and predicted values [26]. Figure 1 depicts the contour plots showing the predicted effects, based on the generated model (eq. 2), of the silicon to zirconium molar ratio (X_1) and the gel ageing

temperature (X_3) at the three levels of HCl (X_2) in the catalytic transesterification of crude palm oil with methanol. As shown, with regards to the initial Zr loading, higher yields towards FAME are predicted when using low silicon to zirconium molar ratios, i.e. high Zr loading in synthesis. This effect could be easily attributed to the fact that higher metal loadings lead to a higher population of potential supported active catalytic sites, causing an overall increase of the catalytic activity of the final materials. In the case of the ageing temperature, higher FAME yields are also predicted for the higher values of the experimental ageing temperature range, whereas an increasing of the HCl concentration in the synthesis media undoubtedly leads to a reduction of the catalytic activity.

The observed trends must be explained attending to the influence exerted by the synthesis variables on the physicochemical properties of the Zr-SBA-15 materials (zirconium content and textural properties, included in Table 4). It must be noted that acid properties can be conditioned by the final zirconium loading as well as the speciation thereof. In this sense, it has been reported that strong Lewis acid sites are dominant when zirconium species are supported as isolated metal sites in a silica matrix [27]. Likewise, the effect of the synthesis pH (through the concentration of HCl) on the incorporation of metals to SBA-15 materials is well known and it has been widely reported for analogue materials [28]. Thus, for the highest HCl concentrations lower Zr loadings are achieved. The reason for this behaviour could be found in the low stability of the forming Zr-O-Si bonds under more acidic conditions. On the other hand, the temperature of the hydrothermal ageing step displays a dramatic influence on the textural properties of the final Zr-SBA-15 materials: it leads to great variations not only on the available surface area and pore volume but also on the mean pore size [25].

Furthermore, the ageing temperature also affects the final form of supported zirconium species. The detection of intense high-angle diffraction signals in the XRD pattern (not shown) recorded for samples aged at 130ºC (Table 4, samples 8, 11 and 18) is indicative of the presence of a crystalline phase. The location of the observed diffractions matches with some of the X-ray diffraction signals described for crystalline zirconium silicate (zircon) [29], especially if zircon is prepared through hydrothermal crystallization [30]. Zircon can be considered as an inactive phase of supported zirconium as it is inferred from the low yield to FAME (27 mol%) achieved in and equivalent reaction assay conducted in the presence of commercial zirconium silicate (Aldrich) as catalyst. This value is similar to that achieved for a blank reaction in the absence of catalyst, confirming the inactivity of such crystalline species. Therefore, we attribute the beneficial effect of increasing ageing temperature to the generation of larger pore sizes, which reduces the limitations to mass transfer, rather than to the formation of different Zr species. In conclusion, high ageing temperature values lead to expanded pore size, whereas low Si:Zr molar ratios and/or low HCl concentrations increase the amount of supported zirconium species onto the mesostructured materials. However, high Zr loadings do not necessarily imply the enhancement of the catalytic activity, since part of this zirconium is incorporated forming the non-active zircon phase (compare for instance samples 7 and 8, Table 4). The evaluation of the acid loading present in final samples is rather clarifying at this point. Thus, sample 8 (Table 4), displaying the highest metal loading among the presented materials, does not display the highest acid loading value, because most of supported zirconium species are, in this case, in the form of zirconia and zirconium silicate, being both species non-acidic materials. A deeper insight in the effect of the different synthesis

variables on the generation of acid sites allows determining the beneficial effect of a HCl low concentration in the synthesis medium. This is, as previously mentioned, not only beneficial for the incorporation of zirconium, but also for the generation of the acid sites. In this way, Zr-SBA-15 materials with high acid loadings display a higher catalytic activity, though, as previously stated, first of all, pore size has to be large enough to avoid hindered access to the catalytic acid sites present in the mesopores. See for instance samples 17 and 18, showing similar acid loadings but very different catalytic activity because of the large differences in the mean pore size. In this way, synthesis conditions that allow maximizing the pore size as well as the acid loading in the final materials should lead to the optimum Zr-SBA-15 catalyst for the catalytic methanolysis of crude palm oil.

Applying the mathematical model (eq. 2), the maximal predicted value for the yield towards FAME within the experimental region is 70.3 mol%. This optimal value corresponds to a Zr-SBA-15 catalyst prepared under the following synthesis conditions: 10 silicon to zirconium molar ratio, 0.63 N HCl concentration in synthesis media, and 130ºC gel ageing temperature (X_1 = -1, X_2 = -0.74 and X_3 = +1, in coded values). These optimal synthesis conditions were used for the preparation of a zirconium-functionalized SBA-15 sample. As expected, the material prepared under such optimized conditions displays both high zirconium incorporation (8.4 wt%) and large textural properties (556 m^2/g BET surface; 1.35 cm^3/g pore volume; and 129 Å mean pore diameter). Figure 2A shows the N_2 adsorption-desorption isotherm of this sample and the type-IV isotherm reveals a low nitrogen uptake at low partial pressures, indicating a minor contribution of the microporosity, and very high total pore volume at high p/p^0 values. Most of the pore volume is readily accessible via large-sized

mesopores (Figure 2B). The so-prepared material also displays excellent mesoscopic ordering as it is inferred from the very intense low angle X-ray diffractions (Figure 2C). Finally, the above-mentioned formation of crystalline zirconium silicate when ageing at 130ºC is also observed in this sample by the detection of the corresponding high-angle X-ray diffractions (Figure 2D). In fact, the presence of such crystalline domains of zirconium silicate is clearly visible in Figure 3, depicting TEM and SEM images. TEM micrograph (Figure 3A) shows the evident ordered hexagonal array of mesopores and no segregation of phases. EDS spot beam analysis all over the ordered Zr-SBA-15 particles revealed a mean Zr content (Si:Zr=20) slightly lower than that detected by ICP-OES bulk analysis (Si:Zr=16), suggesting that most of the zirconium is homogeneously dispersed on the surface, being responsible for the catalytic activity of the material. At lower magnification (SEM image, Figure 3B) a few scarce spherical dense particles (1 μm sized) become visible. EDS analysis on these spheres reveals a high local Zr content, with a silicon to zirconium molar ratio close to 1.0 (that of zirconium silicate). As above mentioned, zirconium silicate is inactive in transesterification so that its presence in the catalysts, consequence of the high ageing temperature, does not affect the overall catalytic performance.

Finally, the optimized Zr-SBA-15 material has been used as catalyst in the methanolysis of crude palm oil with methanol to assess its actual catalytic behavior (reaction conditions were identical to those used in the optimization study included in Table 4). The obtained result reproduces fairly well the yield to FAME predicted by eq. 2 at the optimal synthesis conditions, 70.0 mol% experimental vs. 70.3 mol% predicted, confirming the goodness of the model.

3.2. Optimization of reaction conditions

Once the synthesis conditions for Zr-SBA-15 catalyst were optimized to enhance the catalytic activity in FAME production, the study was focused on the optimization of the reaction conditions. Reaction temperature (X_4), catalyst loading (X_5) and methanol to oil molar ratio (X_6) were used as experimental factors. Results corresponding to the central composite experimental design are shown in Table 5 and the corresponding quadratic model is expressed by equation 3, where only significant (at 95% confidence level) factors and interactions have been included.

$$Y = 70.03 + 6.68 \cdot X_4 + 11.34 \cdot X_5 + 6.31 \cdot X_6 - 3.34 \cdot X_4^2 - 6.21 \cdot X_4 \cdot X_5 + 4.64 \cdot X_4 \cdot X_6 - 2.45 \cdot X_5^2 - 1.13 \cdot X_6^2 \quad \text{(eq. 3)},$$

where Y is the response and represents the Yield to FAME expressed as mol%. The coded independent factors (X_i) adopt values between -α and +α corresponding to the analyzed ranges, being α = ±1.68 (star points). ANOVA of the quadratic regression model demonstrated that it is adequate to explain the experimental results. Likewise, the high value of the regression coefficient, r^2 = 0.9747, indicated a good correlation between the predicted and experimental data. The analysis of the model confirms that the yield to FAME is affected by the main three factors and their respective second order terms. Besides, significant interactions were found between the temperature and the methanol to oil molar ratio, and between the temperature and the catalyst loading. In fact, we reported similar interactions for the same system using a sulfonic acid-modified mesostructured silica catalyst [31]. This means that all the assayed reaction variables exert, as a general term, a positive influence on the production of FAME. Figure 4 depicts contour plots of the response surfaces generated from the mathematical model (eq. 3) showing the effect of temperature (X_4) and catalyst

loading (X_5), for different methanol to oil molar ratios, on the predicted yield to FAME (Y) for the methanolysis of crude palm oil using the optimized Zr-SBA-15 material. Though the effect of all the three studied factors is positive, the crossed effects exert also a significant influence. For instance, increasing the catalyst loading and reaction temperature to the maximum experimental values seems to be excessive, as no further improvement of the FAME yield is achieved. This is attributed to side reactions like the hydrolysis of fatty acid methyl esters. Note that there are significant amounts of water in the reaction media as a consequence of the esterification of the starting free fatty acids (acid value 21.45 mg_{KOH}/g for the crude palm oil used, Table 1, which roughly represents 10 wt% FFA content). Said side reactions become increasingly significant at higher temperatures and catalysts loadings, limiting the overall yield to FAME.

Applying the mathematical model represented by eq. 3, the maximal predicted value for the yield to FAME within the experimental region is 85.1 mol%. This optimal value corresponds to the following reaction conditions: 209ºC, 12.45 wt% catalyst, and 45.80 methanol to oil molar ratio (X_4=+0.30, X_5=+0.49, and X_6=+1.58 in coded values). A catalytic experiment carried out under such reaction conditions provided 84.7% yield to FAME after 3 h of reaction, in fair agreement with the model prediction. Additionally, aiming to evaluate the stability in operation of Zr-SBA-15 catalyst, recycling tests were conducted at the optimized reaction conditions with the optimized catalyst. Figure 5A displays the reaction results for the reutilization experiments. In the first four runs, catalyst recovery between consecutive experiments was carried out by simply filtering and washing with a mixture of *n*-hexane and methanol (in order to remove reactants and reaction products from the pore structure

of the catalyst). As shown, this procedure of intermediate washing is not completely effective in recovering the initial catalytic activity, since a gradual reduction of FAME yield after each run is visible. This fact is probably due to the formation of deposits of polar organic matter over the catalytic centres of Zr-SBA-15, as previously reported by other authors [11], which cannot be removed by the double washing with *n*-hexane and methanol. Such deposits are believed to come primarily from the unsaponifiable fraction of the oil (consisting of substances non-volatile at 100-105ºC obtained by extraction with an organic solvent from the assayed sample after saponification), which in the case of crude palm oil accounts for 2.5 wt% of the starting oil. A thermogravimetric analysis performed on the Zr-SBA-15 catalyst after reaction and double washing (not shown) confirmed the presence of a significant amount of organic matter strongly retained on the catalyst (with a desorption temperature in the TG range of 250-500ºC). Regeneration of the catalyst was therefore proposed by means of thermal degradation of the organic deposits. The choice of the conditions for such a thermal treatment was limited by the calcination procedure used during the synthesis of the catalyst, 450ºC for 5h in air, since the use of higher temperatures might lead to a modification of the textural properties of the catalysts or the speciation of zirconium atoms. Thus, such a thermal treatment led to a full recovery of the starting activity of the Zr-SBA-15 catalyst. This confirms the reversibility of the deactivation as the organic deposits are burnt out upon calcination in air. On the other hand, Fig. 5B shows the kinetic curve for the transesterification of crude palm oil with methanol under the optimized conditions, evidencing that FAME yield keeps increasing with time up to 6 h reaching values over 94 mol%.

3.3. Catalytic transesterification of low-grade raw materials

The catalytic behaviour of the optimized Zr-SBA-15 material was also explored in the production of biodiesel, under the optimal reaction conditions, from low-grade vegetable oils and fats as alternative feedstocks. For this purpose, waste cooking oil (WCO), category-1 fat, pig lard and an animal fats mixture (chicken, pig and beef fats) were assayed. Crude palm oil, previously employed as substrate in the already described optimization studies, was used as reference for comparison purposes. Figure 6 displays the FAME yield achieved from the catalytic experiments carried out for the different feedstocks after 6 hours of reaction. It is noteworthy the outstanding catalytic activity (over 90 mol% in every case) displayed by the Zr-SBA-15 material for every raw material, regardless of its origin or the level of any of the evaluated impurities. Importantly, the catalyst gave again the same FAME yield for every feedstock after 3 hours of reaction, ca. 80 mol% in this case, which demonstrates that the kinetics is not significantly influenced by the presence of the analyzed impurities.

Furthermore, the regenerability of the catalyst by calcinations at 450ºC is confirmed again for every oily feedstock (Fig. 6). Specially remarkable is the conversion achieved with category-1 fat, even in a second use of the catalyst, since this raw material presents exceptionally high levels of acid value (33.45 mgKOH/g), unsaponifiable matter (22.6 wt%), and metals (see Table 1). Such impurities have been proven before to deeply alter the activity of other heterogeneous acid catalysts such as sulfonic acid-modified mesostructured silicas [32]. Fig. 7 depicts the acid values obtained by titration for the starting feedstock and for the respective produced FAME phase after reaction under the optimized conditions. In this case, acid value is directly related to the amount of FFAs within the titrated sample. As shown, a significant

decrease in the acidity is observed for every material (except for lard, where the values are already very low in the feedstock). Specially remarked is the drop in acid value for crude palm oil and category 1 fat, showing very high FFA contents. This is an evidence of the high activity of the catalyst also in the esterification reaction of free fatty acids with methanol.

Therefore, Zr-SBA-15 is shown as a robust and highly active catalyst in the simultaneous esterification of FFAs and transesterification of triglycerides with methanol for low-grade oils and fats, independently of their acid value or unsaponifiable matter content.

4. Conclusions

The double optimization through factorial design of experiments of the synthesis conditions (ageing temperature, hydrochloric acid concentration and Si:Zr molar ratio) of Zr-SBA-15 materials and the operating conditions (reaction temperature, catalyst loading and methanol to oil molar ratio) for biodiesel production is effective to enhance the catalytic activity of these heterogeneous acid catalysts. Optimized synthesis conditions allowed the preparation of a Zr-SBA-15 material showing high metal loading and large textural properties values, which, under the optimized reaction conditions, was able to drive the transesterification of crude palm oil with methanol to achieve 85 mol% FAME yield in 3 h and 92 mol% after 6 h. Moreover, the optimal Zr-SBA-15 material displayed not only high catalytic activity but also very good stability, being reusable for several recycling tests and fully regeneratable by calcination at 450ºC in air. Finally, the catalytic performance of this material was also assessed using low-grade feedstocks containing different amounts of

FFAs, water, alkaline metals or unsaponifiable matter. Zr-SBA-15 material was able to convert these feedstocks in a very similar manner regardless of the presence and concentration levels of the measured impurities, confirming the stability and robustness of this catalyst.

Acknowledgements

Financial supports by Spanish Government-MICINN (project CTQ2008-01396) and Regional Government of Madrid through the project S2009-ENE1743 are gratefully acknowledged. RSV thanks the Spanish Ministry of Science and Innovation (MICINN) for a FPI grant.

References

[1] (a) Y. Zhang, M. Dubé, D. McLean, M. Kates, Bioresour. Technol. 89 (2003) 1. (b) Z.J. Predojević, Fuel 87 (2008) 3522.

[2] M. Canakci, J. van Gerpen, Trans ASAE 44 (2001) 1429.

[3] (a) M.P. Dorado, E. Ballesteros, J.A. Almeida, C. Schellert, H.P. Lohrlein, R. Krause, Trans ASAE 45 (2002) 525. (b) M. Kee Lam, K. Teong Lee, A. Rahman Mohamed, Biotechnol. Adv. 28 (2010) 500.

[4] (a) J.M. Marchetti, V.U. Miguel, A.F. Errazu, Renewable Sustainable Energy Rev. 11 (2007) 1300. (b) A. Demirbas, Energy Convers. Manage. 49 (2008) 125.

[5] (a) J.A. Melero, J. Iglesias, G. Morales, Green Chem. 11 (2009) 1285. (b) S. Semwal, A.K. Arora, R.P. Badoni, D.K. Tuli, Bioresour. Technol. 102 (2011) 2151.

[6] (a) S. Furuta, H. Matsuhashi, K. Arata, Catal. Commun. 5 (2004) 721. (b) C. Martins García, S. Teixeira, L. Ledo Marciniuk, U. Schuchardt, Bioresour. Technol. 99 (2008) 6608. (c) G. Fu, L. Gao, L. Niu, R. Wei, G. Xiao, Energy Fuels 23 (2009) 569. (d) M.K. Lam, K.T. Lee, Fuel 89 (2010) 3866.

[7] (a) Y.M. Park, D.W. Lee, D.K. Kim, J.S. Lee, K.Y. Lee, Catal. Today 131 (2008) 238. (b) S. Furuta, H. Matsuhashi, K. Arata, Biomass Bioenergy 30 (2006) 870. (c) M. Kim, C. DiMaggio, S.L. Yan, H.L. Wang, S.O. Salley, K.Y.S. Ng, Bioresour. Technol. 102 (2011) 2380. (d) C. García-Sancho, R. Moreno-Tost, J.M. Mérida-Robles, J. Santamaría-González, A. Jiménez-López, P. Maireles-Torres, Appl. Catal., B 108-109 (2011) 161.

[8] (a) M.G. Kulkarni, R. Gopinath, L.C. Meher, A.K. Dalai, Green Chem. 8 (2006) 1056. (b) F. Chai, F. Cao, F. Zhai, Y. Chen, X. Wang, Z. Su, Adv. Synth. Catal. 349 (2007) 1057.

[9] (a) I.K. Mbaraka, K.J. McGuire, B.H. Shanks, Ind. Eng. Chem. Res. 45 (2006) 3022. (b) S.M. de Rezende, M. de Castro, M. Garcia, P.L. Silva Jr., F.M.B. Coutinho, R.A. da Silva, E.R. Lachter, Appl. Catal. A 349 (2008) 198. (c) J.A. Melero, L.F. Bautista, G. Morales, J. Iglesias, D. Briones, Energy Fuels 23 (2009) 539.

[10] (a) J. Ni, F.C. Meunier, Appl. Catal. A 333 (2007) 122. (b) J. Jitputti, B. Kitiyanan, P. Rangsunvigit, K. Bunyakiat, L. Attanatho, P. Jenvanitpanjakul, Chem. Eng. J. 116 (2006) 61.

[11] A.C. Alba-Rubio, F. Vila, D. Martín Alonso, M. Ojeda, R. Mariscal, M. López Granados, Appl. Catal. B 95 (2010) 279.

[12] (a) M.D. Gracia, A.M. Balu, J.M. Campelo, R. Luque, J.M. Marinas, A.A. Romero, Appl. Catal. A 371 (2009) 85. (b) A. Jiménez-López, I. Jiménez-Morales, J. Santamaría-González, P. Maireles-Torres, J. Mol. Catal. A: Chem. 335 (2011) 205.

[13] J. Dhainaut, J.P. Dacquin, A.F. Lee, K. Wilson, Green Chem. 12 (2010) 296.

[14] (a) B.L. Newalkar, J. Olanrewaju, S.J. Komarneni, J. Phys. Chem. B 105 (2001) 8356. (b) K. Szczodrowski, B. Prélot, S. Lantenois, J. Zajac, M. Lindheimer, D. Jones, A. Julbe, A. van der Lee, Microporous Mesoporous Mater. 110 (2008) 111.

[15] (a) S.Y. Chen, L.Y. Jang, S. Cheng, Chem. Mater. 16 (2004) 4174. (b) Y. Du, S. Liu, Y. Zhang, F. Nawaz, Y. Ji, F.S. Xiao, Microporous Mesoporous Mater. 121 (2009) 185. (c) S.Y. Chen, L.Y. Jang, S. Cheng, J. Catal. 270 (2010) 196.

[16] (a) L. Fuxiang, Y. Feng, L. Yongli, L. Ruifeng, X. Kechang, Microporous Mesoporous Mater. 101 (2007) 250. (b) V. Degirmenci, Ö.F. Erdem, O. Ergun, A. Yilmaz, D. Michel, D. Uner, Top. Catal. 49 (2008) 204. (c) K. Szczodrowski, B. Prélot, S. Lantenois, J.M. Douillard, J. Zajac, Microporous Mesoporous Mater. 124 (2009) 84.

[17] J. Iglesias, J.A. Melero, L.F. Bautista, G. Morales, R. Sánchez-Vázquez, M.T. Andreola, A. Lizárraga-Fernández, Catal. Today 167 (2010) 46.

[18] J.A. Melero, J.M. Arsuaga, P. de Frutos, J. Iglesias, J. Sainz, S. Blázquez, Microporous Mesoporous Mater. 86 (2005) 364.

[19] J. Iglesias, M.D. Gracia, R. Luque, A.A. Romero, J.A. Melero, ChemCatChem 4 (2011) 379-386.

[20] G.E.P. Box, K.B.J. Wilson, Roy. Stat. Soc. B Stat. Meth. 13 (1951) 1.

[21] C. Plank, E. Lorbeer, Fat Sci. Technol. 96 (1994) 379-386.

[22] R. van Grieken, G. Calleja, G.D. Stucky, J.A. Melero, R.A. García, J. Iglesias, Langmuir 19 (2003) 3966.

[23] G. Gelbard, O. Brès, R.M. Vargas, F. Vielfaure, U.F. Schuchardt, J. Am. Oil Chem. Soc. 72 (1995) 1239.

[24] J.H. Toney, T.J. Marks, J. Am. Chem. Soc. 107 (1985) 947.

[25] (a) T. Klimova, A. Esquivel, J. Reyes, M. Rubio, X. Bokhimi, J. Aracil, Microporous Mesoporous Mater. 93 (2006) 331. (b) D. Pan, P. Yuan, L. Zhao, N. Liu, L. Zhou, G. Wei, J. Zhang, Y. Ling, Y. Fan, B. Wei, H. Liu, C. Yu, X. Bao, Chem. Mater. 21 (2009) 5413.

[26] D.C. Montgomery, Design and Analysis of Experiments; John Wiley and Sons: New York, 2005.

[27] A. Ramanathan, M.C. Castro-Villalobos, C. Kwakernaak, S. Telalovic, U. Hanefeld, Chem. Eur. J. 14 (2008) 961.

[28] (a) S. Wu, Y. Han, Y.C. Zou, J.W. Song, L. Zhao, Y. Di, S.Z. Liu, F.S. Xiao, Chem. Mater. 16 (2004) 486. (b) Z.S. Lou, R.H. Wang, H. Sun, Y. Chen, Y.H. Yang,

Microporous Mesoporous Mater. 110 (2008) 347. (c) M. Selvaraj, Y. Choe, Appl. Catal. A. 373 (2010) 186.

[29] (a) L. Rubio-Puzzo, M.C. Caracoche, M.M. Cervera, P.C. Rivas, A.M. Ferrari, F. Bondioli, J. Solid State Chem. 150 (2000) 14. (b) C. Veytizou, J.F. Quinson, O. Valfort, G. Thomas, Solid State Ionics 139 (2001) 139.

[30] (a) R. Valéro, B. Durand, J.L. Guth, T. Chopin, J. Sol-Gel Sci. Technol. 13 (1998) 119. (b) R. Valéro, B. Durand, J.L. Guth, T. Chopin, Microporous Mesoporous Mater. 29 (1999) 311.

[31] J.A. Melero, L.F. Bautista, J. Iglesias, G. Morales, R. Sánchez-Vázquez, I. Suárez-Marcos, Top. Catal. 53 (2010) 795.

[32] G. Morales, L.F. Bautista, J.A. Melero, J. Iglesias, R. Sánchez-Vázquez, Bioresour. Technol. 102 (2011) 9571.

Table 1. Properties of low-grade oil and fats evaluated as biodiesel feedstocks.

Property	Low-grade lard	Category 1 fat	Mixed fat	Waste cooking oil	Crude Palm Oil
Acid value (mg_{KOH}/g) [a]	0.47	33.45	3.57	4.06	21.45
Metals (mg/kg) [b]					
P	72.6	85.9	302.8	3.1	13.1
Na	n.d.	154.4	83.8	2.8	15.7
K	0.4	144.2	10.8	n.d.	n.d.
Mg	0.4	0.1	10.8	n.d.	4.9
Ca	4.5	2.6	123.3	0.5	5.3
Fatty acid profile (wt%) [c]					
Myristic acid (14:0)	1.4	3.1	2.1	0.2	0.8
Palmitic acid (16:0)	26.6	28.1	26.6	9.3	43.3
Palmitoleic acid (16:1)	3.0	0.0	3.4	0.5	0.0
Stearic acid (18:0)	14.2	20.0	16.7	3.9	5.2
Oleic acid (18:1)	47.0	41.6	42.1	54.5	39.7
Linoleic acid (18:2)	6.2	6.0	7.6	29.7	10.5
Linolenic acid (18:3)	0.4	0.5	0.57	0.3	0.4
Water (mg/kg) [d]	288	1170	956	1398	687
Unsaponifiables (wt%) [e]	2.9	22.6	9.8	1.0	2.5

Analytical Methods: [a] UNE EN ISO 660:2000; [b] ASTM D5185-05; [c] UNE EN ISO 5508:1996 and 5509:2000; [d] UNE EN ISO 12937:2001; [e] Method reported by Plank and Lorbeer, 1994 [21]. n.d.: not detected (below detection limit).

Table 2. Range and levels of the factors for the optimization of the synthesis variables.

Factor	Coded levels		
	-1	0	+1
X_1: Silicon to zirconium molar ratio	10:1	20:1	30:1
X_2: Hydrochloric acid concentration (N)	0.5	1.0	1.5
X_3: Ageing temperature (ºC)	70	100	130

Table 3. Range and levels of the factors for the optimization of the reaction conditions.

Factor	Coded levels				
	-α (-1.68)	-1	0	+1	+α (+1.68)
X_4: Reaction temperature (ºC)	149.6	170	200	230	250.4
X_5: Catalyst loading (wt%)	1.6	5	10	15	18
X_6: Methanol to oil molar ratio (MR)	13:1	20:1	30:1	40:1	47:1

Table 4. Full factorial face-centred central composite design matrix of three variables along with the observed responses for the optimization of the synthesis of Zr-SBA-15.

Sample	Experimental factors			FAME yield [d] (mol%)	Zr [e] (wt%)	Acid loading [f] (meq/g)	Textural properties			
	X_1 [a]	X_2 [b]	X_3 [c]				S_{BET} [g] (m^2/g)	V_P [h] (cm^3/g)	Dp [i] (Å)	Wt [j] (Å)
1	0	0	0	62.6	6.7	0.290	806	1.27	96	33
2	0	0	0	61.3	5.6	0.287	808	1.24	95	25
3	0	0	0	61.1	5.7	0.286	826	1.29	97	29
4	0	0	0	65.8	4.7	0.293	821	1.26	96	30
5	-1	+1	-1	52.4	4.8	0.141	978	1.05	75	54
6	-1	-1	-1	53.8	8.0	0.133	870	0.98	91	49
7	-1	-1	+1	69.7	3.9	0.213	471	1.16	111	12
8	-1	+1	+1	61.0	11.0	0.239	546	1.38	127	5
9	+1	+1	-1	46.9	3.1	0.153	997	1.09	75	51
10	+1	-1	-1	47.8	4.2	0.241	839	0.80	64	56
11	+1	-1	+1	63.0	8.5	0.273	506	1.24	118	11
12	+1	+1	+1	61.1	4.5	0.222	557	1.25	119	12
13	-1	0	0	68.0	8.2	0.206	643	1.10	93	25
14	+1	0	0	56.3	4.3	0.234	870	1.28	91	27
15	0	-1	0	60.5	5.6	0.235	777	1.22	95	26
16	0	+1	0	56.1	4.7	0.198	701	1.05	87	34
17	0	0	-1	53.7	5.1	0.231	925	0.95	69	39
18	0	0	+1	64.3	7.2	0.239	469	1.14	114	12

[a] Coded Si:Zr molar ratio; [b] Coded HCl concentration; [c] Coded gel ageing temperature; [d] Reaction with crude palm oil under the following conditions: 200ºC, 10 wt% catalyst loading, 30:1 methanol to oil molar ratio, 3 hours; FAME yield calculated from ^{1}H NMR experiments; [e] Zr loading on final materials measured by means of ICP-OES; [f] Acidity measured by NH_3 TPD experiments; [g] Total surface area; [h] Total pore volume recorded at p/p_0=0.985; [i] Mean pore size calculated by the BJH method applying the KJS correction; [j] Pore wall thickness evaluated as a_0-D_p.

Table 5. Full factorial central composite design matrix of three variables along with the observed responses for the optimization of reaction conditions using the optimized Zr-SBA-15 catalyst.[a]

Reaction	Experimental factors						FAME yield (mol%)
	Coded			Real			
	X_4	X_5	X_6	Temp. (ºC)	Cat. loading (wt%)	MeOH to oil molar ratio	
1	0	0	0	200	10	30:1	70.6
2	0	0	0	200	10	30:1	68.5
3	0	0	0	200	10	30:1	70.0
4	0	0	0	200	10	30:1	70.9
5	+1	+1	+1	230	15	40:1	84.5
6	-1	-1	-1	170	5	20:1	38.1
7	+1	+1	-1	230	15	20:1	60.4
8	+1	-1	+1	230	5	40:1	77.0
9	+1	-1	-1	230	5	20:1	55.4
10	-1	+1	+1	170	15	40:1	73.5
11	-1	+1	-1	170	15	20:1	69.6
12	-1	-1	+1	170	5	40:1	42.9
13	0	+α	0	200	18	30:1	87.6
14	0	-α	0	200	1.6	30:1	39.8
15	0	0	+α	200	10	47:1	76.9
16	0	0	-α	200	10	13:1	58.0
17	+α	0	0	250.4	10	30:1	72.5
18	-α	0	0	149.6	10	30:1	49.9

[a] Transesterification of crude palm oil with methanol. Reaction time 3 h. FAME yield calculated from ^{1}H NMR experiments.

Figure and Scheme captions

Figure 1. Contour plots showing the predicted effect of silicon to zirconium molar ratio (X_1) and ageing temperature (X_3) on the yield to FAME (Y) for the methanolysis of crude palm oil using Zr-SBA-15 catalysts at the three evaluated levels of HCl concentration. Reaction conditions: 200ºC, 10 wt% catalyst loading, 30:1 methanol to oil molar ratio, 3 h reaction time.

Figure 2. (A) Nitrogen adsorption-desorption isotherm; (B) Pore size distribution; (C) Low angle XRD pattern and (D) High angle XRD pattern recorded for a Zr-SBA-15 material prepared under optimized synthesis conditions.

Figure 3. (A) Transmission electron microphotograph, (B) Scanning electron microphotograph; and the corresponding EDX analyses of Zr-SBA-15 material prepared under optimized synthesis conditions.

Figure 4. Contour plots showing the predicted effect of reaction temperature (X_4) and catalyst loading (X_5) on the yield to FAME (Y) for the methanolysis of crude palm oil using the optimized Zr-SBA-15 catalysts at three different levels of methanol to oil molar ratio (MR). Reaction time: 3 h.

Figure 5. (A) Catalyst recycling tests with 3 h reaction time. (B) Evolution of the yield to FAME with the reaction time. Reaction conditions: 209ºC, 45.80 methanol to oil molar ratio, 12.45 wt% catalyst loading. Optimized Zr-SBA-15 catalyst.

Figure 6. FAME yield from low-grade feedstocks using the optimized Zr-SBA-15 catalyst and catalyst recycling after calcination at 450ºC. Reaction conditions: 209ºC, 45.80 methanol to oil molar ratio, 12.45 wt% catalyst loading, 6 h reaction time.

Figure 7. Acid values of the raw materials and the corresponding crude reaction product (FAME phase) obtained over the optimized Zr-SBA-15 catalyst. Reaction conditions: 209ºC, 45.80 methanol to oil molar ratio, 12.45 wt% catalyst loading, 6 h reaction time.

Figure 1

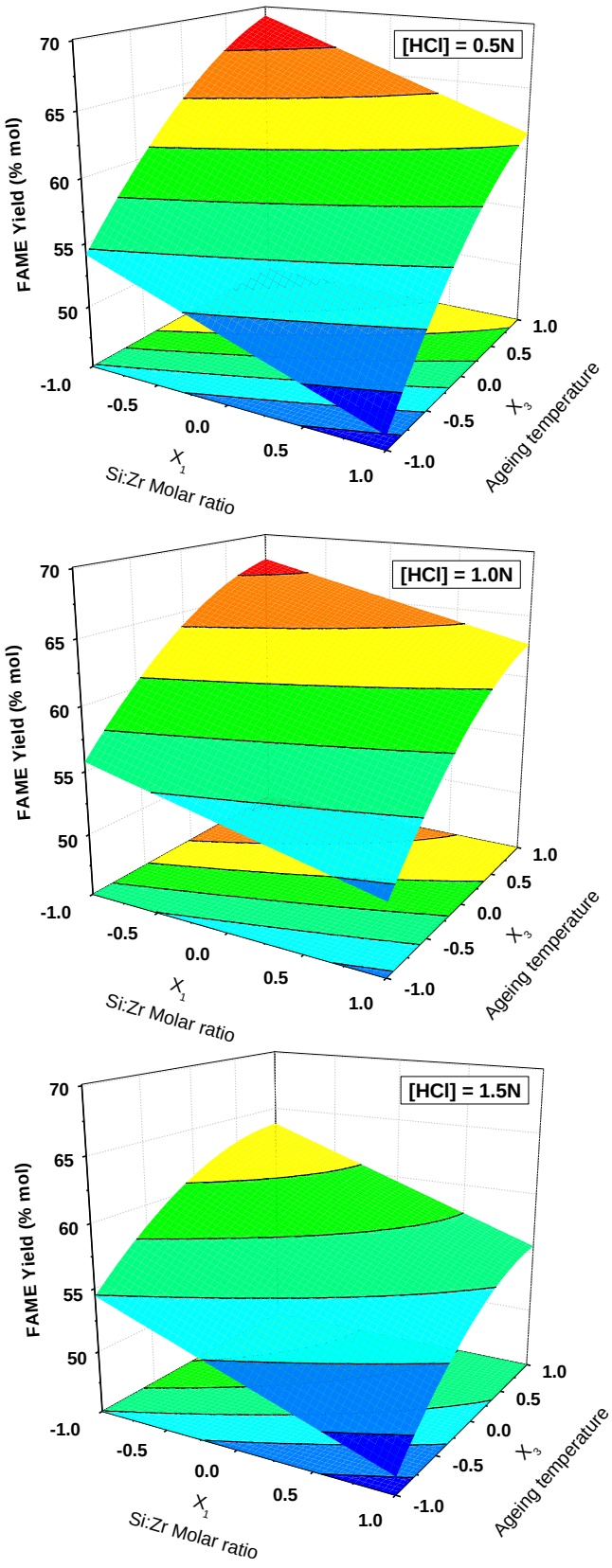
[HCl] = 0.5N
[HCl] = 1.0N
[HCl] = 1.5N
FAME Yield (% mol)
70
65
60
55
50
-1.0
-0.5
0.0
0.5
1.0
X1
Si:Zr Molar ratio
X3
Ageing temperature

Figure 2

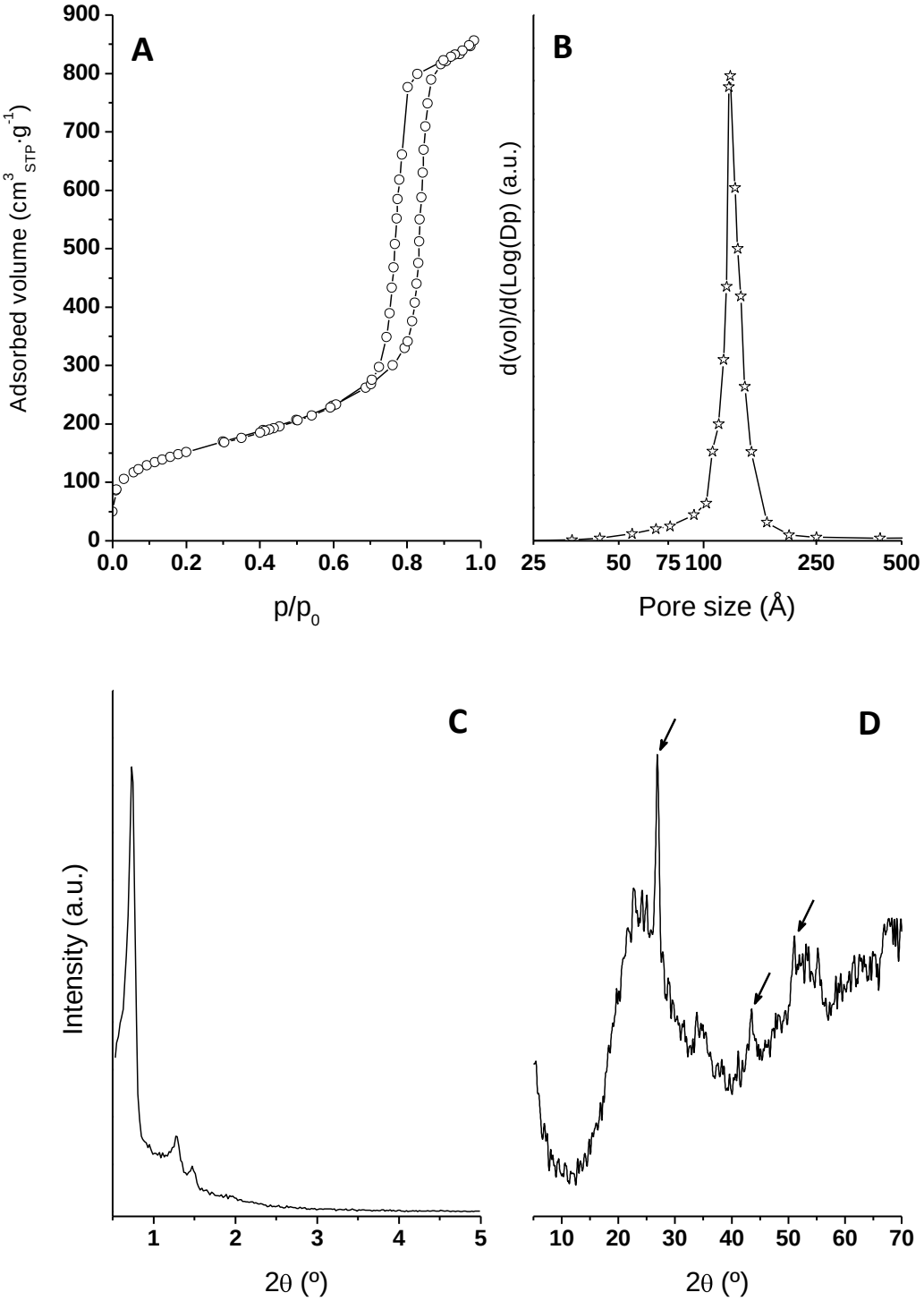
A
B
C
D
Adsorbed volume (cm3 STP.g-1)
p/p0
d(vol)/d(Log(Dp) (a.u.)
Pore size (Å)
Intensity (a.u.)
2θ (º)
2θ (º)

Figure 3

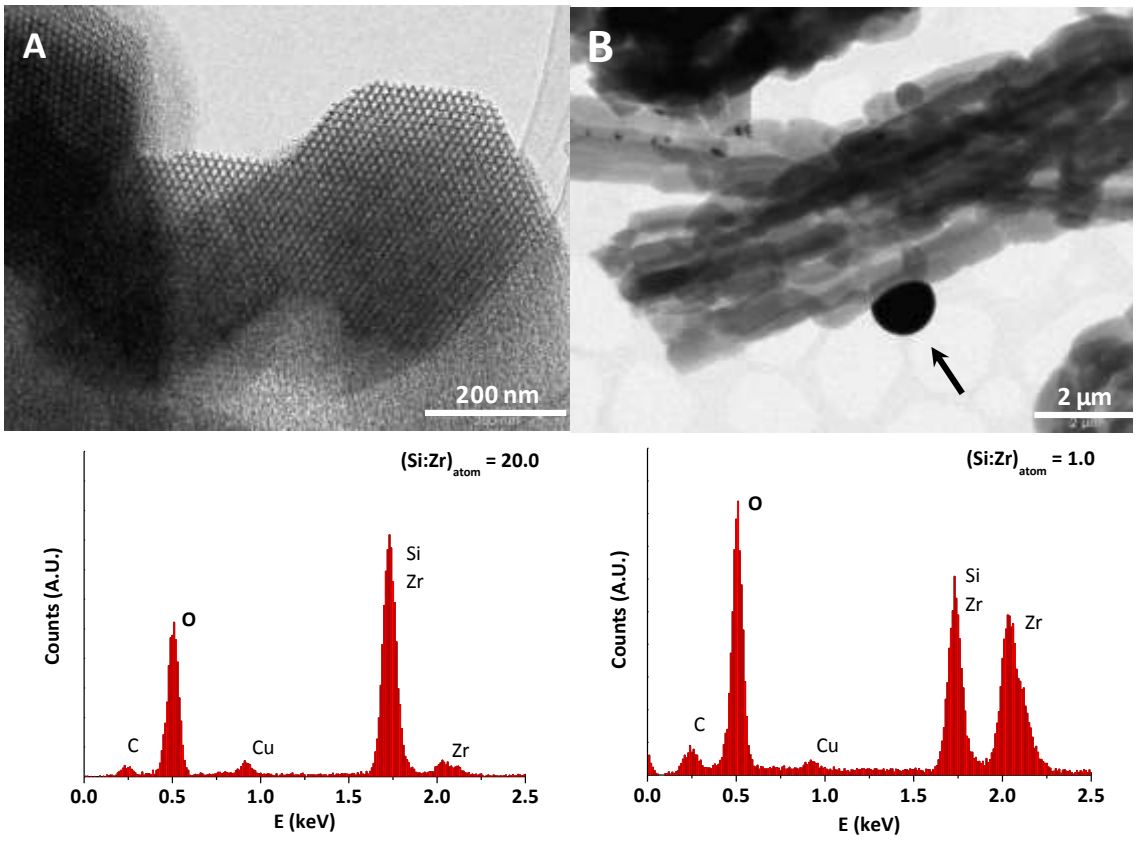
A
200 nm
B
2 µm
(Si:Zr)atom = 20.0
Counts (A.U.)
O
Si
Zr
C
Cu
Zr
0.0
0.5
1.0
1.5
2.0
2.5
E (keV)
(Si:Zr)atom = 1.0
Counts (A.U.)
O
Si
Zr
Zr
C
Cu
0.0
0.5
1.0
1.5
2.0
2.5
E (keV)

Figure 4

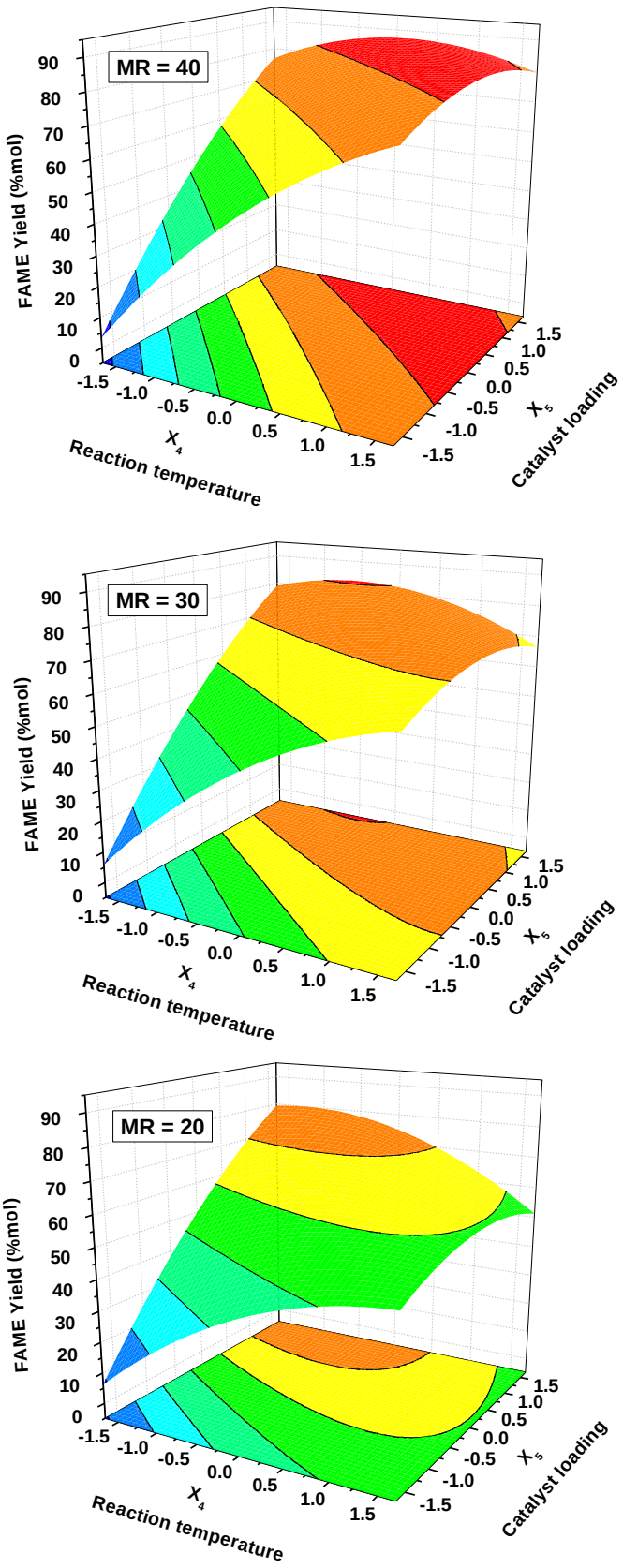
MR = 40
MR = 30
MR = 20
FAME Yield (%mol)
0
10
20
30
40
50
60
70
80
90
-1.5
-1.0
-0.5
0.0
0.5
1.0
1.5
X_4
Reaction temperature
X_5
Catalyst loading

Figure 5

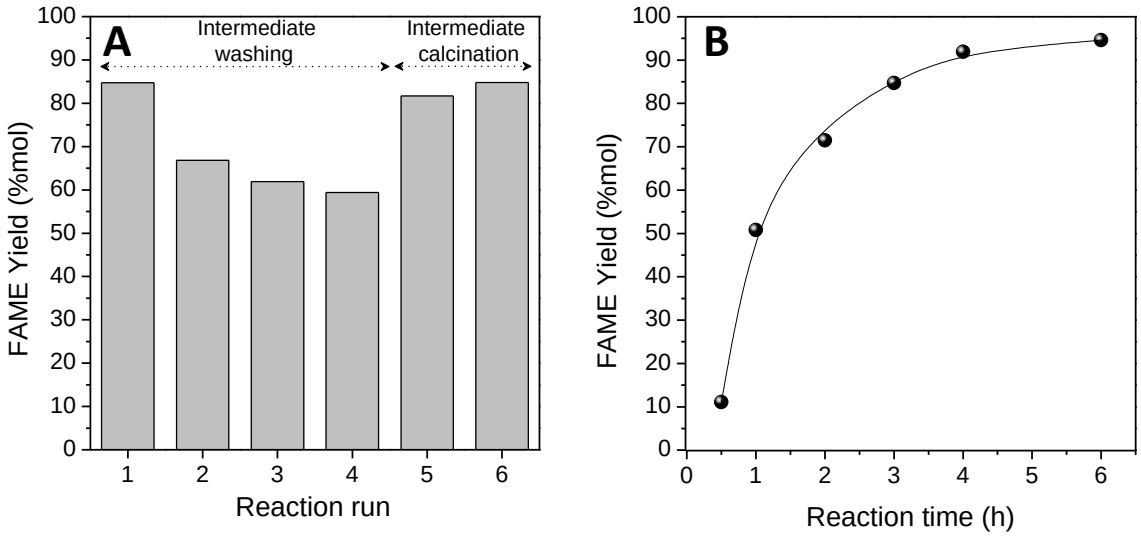
A
Intermediate washing
Intermediate calcination
FAME Yield (%mol)
Reaction run
B
FAME Yield (%mol)
Reaction time (h)

Figure 6

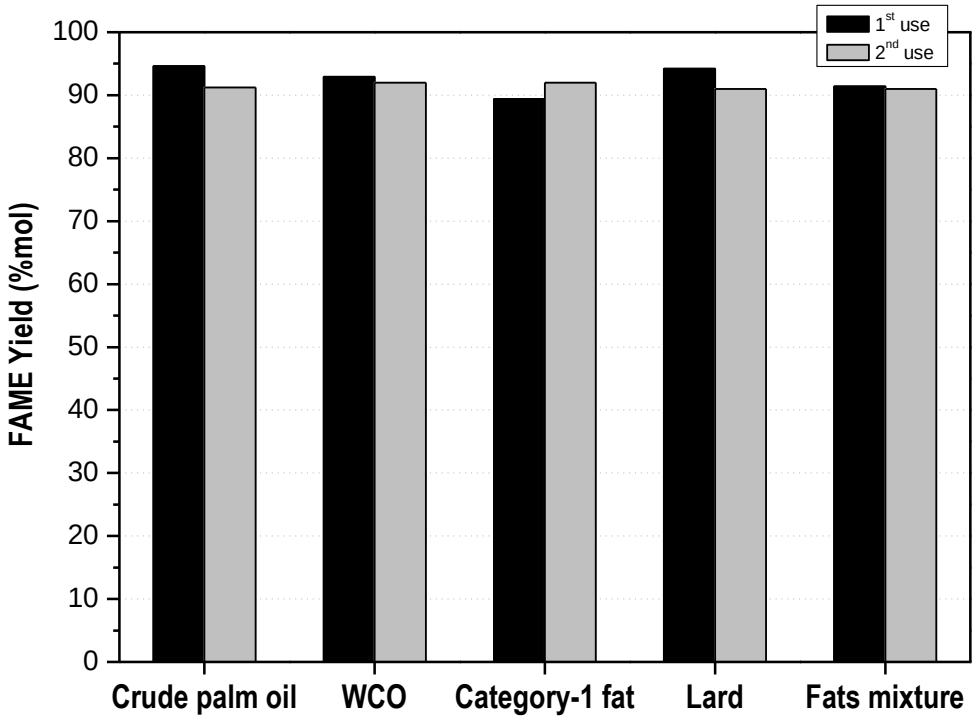
1st use
2nd use
FAME Yield (%mol)
100
90
80
70
60
50
40
30
20
10
0
Crude palm oil
WCO
Category-1 fat
Lard
Fats mixture

Figure 7

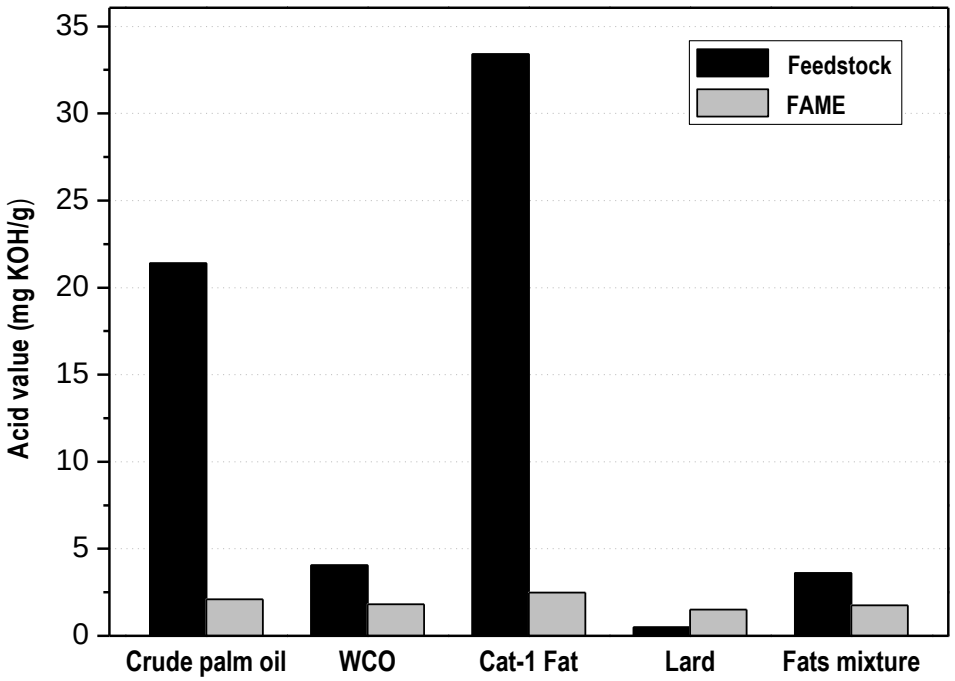
Acid value (mg KOH/g)
35
30
25
20
15
10
5
0
Feedstock
FAME
Crude palm oil
WCO
Cat-1 Fat
Lard
Fats mixture